

Published in final edited form as:

ACS Med Chem Lett. 2011 August 23; 2(11): 798–803. doi:10.1021/ml200125r.

Host-directed Inhibitors of Myxoviruses: Synthesis and in vitro Biochemical Evaluation

Aiming Sun^{*,†}, J. Maina Ndungu[†], Stefanie A Krumm^{§,μ}, Jeong-Joong Yoon^{§,μ}, Pakk Thepchatri[†], Michael Natchus[†], Richard K Plemper^{§,μ,ν}, and James P. Snyder^{†,‡}

[†]Emory Institute for Drug Discovery, Emory University, Atlanta, GA 30322

[§]Department of Pediatrics, Emory University School of Medicine, Atlanta, GA 30322

^μChildren's Healthcare of Atlanta, Atlanta, GA 30322

^ν Department of Microbiology & Immunology, Emory University School of Medicine, Atlanta, GA, 30322

[‡] Department of Chemistry, Emory University, Atlanta, GA 30322

Abstract

Drugs targeted to viral proteins are highly vulnerable to the development of viral resistance. One little explored approach to the treatment of viral diseases is the development of agents that target host factors required for virus replication. Myxoviruses are predominantly associated with acute disease and, thus, ideally suited for this approach since the necessary treatment time is anticipated to be limited. High-throughput screening previously identified benzimidazole 22407448 with broad anti-viral activity against different influenza virus and paramyxovirus strains. Hit to lead chemistry has generated **6p** (JMN3-003) with potent antiviral activity against a panel of myxovirus family members exhibiting EC₅₀ values in the low nanomolar range.

Keywords

Host-directed; non-nucleoside; small molecule inhibitor; influenza virus; myxovirus; benzimidazole

Myxoviruses are responsible for the majority of human morbidity and mortality cases due to viral respiratory illness globally.¹ Influenza virus is the leading cause of these events in North America, although vaccine prophylaxis is widely available. Despite extensive research, no vaccines currently exist for several major pathogens of the paramyxovirus family such as respiratory syncytial virus (RSV) or different human parainfluenzaviruses (HPIVs). Ribavirin (RBV) is a synthetic nucleoside analog with broad-spectrum antiviral activity. Although RBV is approved for the treatment of hepatitis C virus, RSV and Lassa fever virus infections, its efficacy is limited and the drug is compromised by several side effects.² Previously, we utilized high-throughput screening (HTS) to identify small molecule inhibitors against MeV RNA dependent RNA polymerase (RdRp) activity.³ However, viral adaptation has demonstrated that robust resistance to inhibition by these compounds can originate from single point mutations in the targeted viral protein.^{4,5} In an attempt to counteract viral escape from inhibition, we have explored targeting host factors required for

*Corresponding author: Phone: 404-712-8680; Fax: 404-727-6689; asun2@emory.edu.

Supporting Information. Experimental details for the synthesis and characterization of **3-11**, **12**, **13**, **15**, **20** and **21**. Experimental details for biology assays. This material is available free of charge via the Internet at <http://pubs.acs.org>.

viral replication rather than viral proteins directly. Anticipated advantages of this strategy include a decreased frequency of viral escape from inhibition and a broadened pathogen target spectrum. High-throughput screening in combination with counter-screening for a broadened viral target spectrum that extends to other pathogens of the myxovirus families, has identified several antiviral hits that likely target host cells.⁶ This approach yielded several benzimidazoles of the same class (22407448 (BM-1),⁷ 22404943 and 22407466) as well-behaved inhibitors of measles virus (MeV). Potencies (EC₅₀) against MeV are 0.2, 0.7 and 2.1 μ M, respectively. (**Figure 1**) Hit BM-1 in particular is unusual since it shows broad-spectrum antiviral action against various paramyxoviruses in the low micromolar to nanomolar range.⁶

In order to confirm the activity, BM-1 was re-synthesized and re-assayed. For hit confirmation, dose-response curves were generated. Synthesized BM-1 revealed behavior identical to the original library member against CDV, HPIV3 and MeV. In parallel, MTT assays were employed to determine compound-induced cytotoxicity in the absence of viral infection. Synthesis was initiated by coupling of 1-fluoro-2-nitrobenzene **1** with *p*-anisidine **2** in the presence of potassium carbonate to provide N-(4-methoxyphenyl)-2-nitroaniline **3**. Reduction of **3** gave diamine **4**, which was treated with 1,1-thiocarbonyldiimidazole in dichloromethane to afford 1-(4-methoxyphenyl)-1H-benzimidazole-2-thiol **5**. The 2-thioimidazole **5** was transformed to its potassium salt and coupled with 2-bromo-N-(3,5-dichloropyridin-2-yl)propanamide to give BM-1. The approach has been used for the synthesis of a set of BM-1 derivatives, which are described below (**Scheme 1**).

A structure-activity profile has begun to emerge by examination of the three molecular fragments circumscribed in **Figure 2**; namely the benzimidazole (A), the α -thio-amide linker (B) and the substituted pyridine ring (C).

The first stage of hit optimization focused on introducing a variety of aromatic rings as pyridine replacements, since modification of the C sector is achieved in a straight forward fashion by employing the same synthesis methodology utilized for the synthesis of BM-1 (**Scheme 1**). A small and compact library of 30-50 analogs was obtained by utilizing different α -halide amides for the final coupling step. Substituted pyridines, pyrazoles, triazines, thiazoles and other functionalities were used instead of **7**. A second group of analogs was prepared by employing alternative anilines in sector A. The *para*-methoxy group was replaced by hydrogen, ethoxy, fluoro and hydroxyl, among others. Sector C analogs with chloro, methyl and trifluoromethyl substituents show activities very similar to BM-1 (**6a** and **6d**, Table 1). The corresponding ethoxy analog delivers slightly better activity (entry **6c**), while pyrazole and isoxazole replacements furnish 2-fold reduced potency (entries **6j** and **6n**). The fluoro-analog is virtually equipotent to BM-1 (entry **6b**). The thiazole functionality reduces activity by 10-fold (entry **6m**), while triazines are significantly weaker still (entries **6i** and **6k**). However, most of the active compounds listed in Table 1 were toxic in the Trypan blue exclusion assay with CC₅₀ values of 1-10 μ M. The *p*-ethoxy analog is the exception with reduced toxicity at 20 μ M (entry **6c**). Encouragingly, **6p** (JMN3-003) with a substituted phenyl in sector C demonstrated strong antiviral activity (EC₅₀ = 170 nM) against MeV and cell cytotoxicity over 75 μ M (entry **6p**, Table 1). As outlined in the context of the recently reported detailed molecular characterization of JMN3-003, antiviral activities were evaluated using actively dividing cells, while CC₅₀ values were determined for confluent cell populations, thus reflecting acute toxicity. Independent assessment of cell proliferation revealed a cytostatic effect of JMN3-003. This was found, however, not to be the basis for the antiviral effect.⁸ In order to understand the relationship between chirality and potency, R- and S- isomers of **6p** were isolated by chiral HPLC. Both isomers were subjected to the MeV inhibition assay. Potency of the S-isomer was essentially identical to the racemic mixture **6p**, while the antiviral capacity of the R-

isomer was slightly reduced (Table 1). A newly developed methodology for the asymmetric synthesis of both isomers will be reported elsewhere.

For part A of hit modification, we initially tried to replace the fused benzene of the benzoimidazole with pyridine and functionalize the benzene moiety by substitution with Me, Br, or COOEt. Unfortunately, most of the analogs experienced either significant reduction or complete loss of activity. Thus, we didn't pursue this series further.

For replacement of the 2-thioacetamide linker, five different variations of the central tether with an equivalent number of chain atoms were prepared. Compound designations **11-15** (Scheme 2, 3 & 4) and the corresponding activities are recorded in Table 2, illustrating a significant reduction or loss of activity relative to BM-1. Systematic structural modification revealed that substitution of benzyl for phenyl at the benzimidazole *N1* position delivers analogs with similar anti-MeV viral activity. (Figure 2, sector A). Benzyl derivatives **20** and **21** deliver fairly good potency with EC₅₀ at 0.5 μ M and 0.4 μ M, respectively (Table 2). Thus, both derivatives **11** and **13** bear a benzyl group instead of the *p*-methoxy phenyl group as shown in Table 2. Compound **11**, incorporating NH in the central linker, introduces additional hydrogen-bond capacity and a new pK_a center, while **12**, **13**, **14** and **15** (CH₂, O, SO and SO₂, respectively) sustain somewhat different linker geometries by comparison with the sulfur-containing tether of BM-1. The importance of sulfur versus other atoms was also observed during discovery of the HIV reverse transcriptase inhibitor RDEA-806,^{9, 10} which shares the central 2-thio-acetamide linker with BM-1 and has achieved success in clinical trials. (Figure 3) Obviously, a sulfur atom in the linker is essential. However, its precise role at the binding site remains to be fully defined. Comparative conformational searches for otherwise identical analogs with O, NH and CH₂ replacements for S suggest that sulfur is possibly unique in providing an energetically accessible bioactive conformation.¹¹

Analog **11** was prepared as outlined in Scheme 2. 2-Chloro-benzimidazole was treated with *p*-methoxybenzyl bromide in the presence of potassium carbonate to provide chloro-benzimidazole **8**. The latter was coupled with racemic alanine methyl ester in the microwave at 165°C for 1 h to afford 2-aminoimidazole derivative **9**, which was hydrolyzed to the corresponding acid **10**. The latter was treated with oxalyl chloride followed by coupling with 2-chloro-4-methylaniline to furnish the final product **11** (Scheme 2).

The synthesis of carbon analog **12** proceeded from reaction of diamine **4** with succinic anhydride to give the benzimidazole **16**. Hydrolysis of **16** under basic conditions with lithium hydroxide (LiOH) in a mixture of THF and water delivered acid **17**, which was further coupled with 2-chloro-4-methylaniline in the presence of isopropyl chloroformate and 4-methylmorpholine to afford **12** (Scheme 3).

The synthesis of the oxygen analog **13** commenced with the protection of benzyl-L-lactate as a silyl ether, which on hydrogenolysis furnished acid **18**. BOP-mediated coupling of **18** with 2-chloro-4-methylaniline followed by cleavage of the silyl group furnished alcohol **19**. Treatment of **19** with NaH facilitated coupling with 1-benzyl-2-chloro-1H-benzimidazole to afford **13** (Scheme 4).

Sulfoxide analog **14** and sulfone analog **15** can be easily obtained by oxidation of **6p** with 1.0 eq and 2.0 eq of 3-chloroperoxybenzoic acid (MCPBA), respectively.

6p(JMN3-003) is a broadly active anti-myxovirus agent

Benzene analog **6p** has surfaced as the most promising candidate of this compound series with superb antiviral potency and low cytotoxicity. The compound shows potent activity against MeV and a selection of clinically significant members of the para- and

orthomyxovirus families. We also compared the anti-myxovirus activity of **6p** with the previously reported MeV RdRp inhibitor AS-136a. The latter shows high selectivity against MeV, while **6p** exhibits a broad range of anti-myxovirus activities with EC₅₀ values ranging from 10 to 70 nM in virus yield reduction assays depending on the target virus. Detailed biological evaluation and target examination have been reported elsewhere.⁸

In summary, high-throughput screening has identified several hits in the benzimidazole class with potent anti-MeV activities. Follow-up counter-screening assays uncovered BM-1 as a well-behaved inhibitor with the ability to block replication of a broad range of myxovirus family members. By optimization of BM-1, we have developed preliminary SAR within the three pharmacophoric sectors highlighted in **Figure 2**. A variety of structural modifications essentially abolishes antiviral activity or results in high cytotoxicity. Particularly influential for the SAR of these agents are the structural constitutions of the amide substituents and the sulfur atom of the central tether. The most potent analog **6p**, was generated by replacing the pyridine ring in BM-1 with a substituted phenyl ring. The compound shows activity against MeV at 170 nM (viral CPE-reduction assay) and 30 nM (virus yield reduction assay) and does not display any detectable acute cytotoxicity. **6p** was also evaluated for its antiviral activity against a selection of clinical-relevant paramyxovirus (RSV, MuV, and HPIV3) and orthomyxovirus (influenza) family members. The compound exhibits superb inhibitory activity against all the viruses tested with EC₅₀ values ranging from 10 to 70 nM in virus yield reduction assays.⁸ These results demonstrate that **6p** has great potential as a lead for development of host-directed antiviral drugs. Pharmacokinetics evaluation, *in vivo* efficacy and expansion of **6p** library are currently in progress.

Supplementary Material

Refer to Web version on PubMed Central for supplementary material.

Acknowledgments

We are grateful to Dr. Dennis Liotta for generous financial support and scientific discussions. This work was supported, in part, by Public Health Service Grants AI071002 and AI085328 (to R. K. P.) from the NIH/NIAID and by Public Health Service Grant HG003918-02 (to J.P.S.) from the NIH.

References

1. König R, Stertz S, Zhou Y, Inoue A, Hoffmann H-H, Bhattacharyya S, Alamares JG, Tscherne DM, Ortigoza MB, Liang Y, Gao Q, Andrews SE, Bandyopadhyay S, Jesus PD, Tu BP, Pache L, Shih C, Orth A, Bonamy G, Miraglia L, Ideker T, García-Sastre A, Young JAT, Palese P, Shaw ML, Chanda SK. Human host factors required for influenza virus replication. *Nature*. 2010; 463:813–817. [PubMed: 20027183]
2. a Martin P, Jensen DM. Ribavirin in the treatment of chronic hepatitis C. *J. Gastroenterol Hepatol*. 2008; 23:844–855. [PubMed: 18565019] b Dixit NM, Perelson AS. The metabolism, pharmacokinetics and mechanisms of antiviral activity of ribavirin against hepatitis C virus. *Cell Mol Life Sci*. 2006; 63:832–842. [PubMed: 16501888] c Buckwold VE, Wei J, Wenzel-Mathers M, Russell J. Synergistic in vitro interactions between alpha interferon and ribavirin against bovine viral diarrhea virus and yellow fever virus as surrogate models of hepatitis C virus replication. *Antimicrob Agents Chemother*. 2003; 47:2293–2298. [PubMed: 12821481] d Willis RC, Carson DA, Seegmiller JE. Adenosine kinase initiates the major route of ribavirin activation in a cultured human cell line. *Proc. Natl. Acad. Sci. USA*. 1978; 75:3042–3044. [PubMed: 210448]
3. a Sun A, Chandrakumar N, Yoon J-J, Plemper RK, Snyder JP. Nonnucleoside inhibitors of the measles virus RNA-Dependent RNA polymerase activity: Synthesis and in vitro evaluation. *Bioorg. Med. Chem. Lett*. 2007; 17:5199–5203. [PubMed: 17643302] b Sun A, Yoon JJ, Yin Y, Prussia A, Yang Y, Min J, Plemper RK, Snyder JP. Potent non-nucleoside inhibitors of the measles virus RNA-dependent RNA polymerase complex. *J. Med. Chem*. 2008; 51:3731–3741. [PubMed: 18565019]

- 18529043] c White LK, Yoon J-J, Lee JK, Sun A, Du Y, Fu H, Synder JP, Plemper RK. Nonnucleoside inhibitor of measles virus RNA-dependent RNA polymerase complex activity. *Antimicrob. Agents Chemother.* 2007; 51:2293–2303. [PubMed: 17470652]
4. Yoon J-J, Krumm SA, Ndungu JM, Hoffman V, Bankamp B, Rota PA, Sun A, Snyder JP, Plemper RK. Target Analysis of the experimental measles therapeutic AS-136a. *Antimicrob. Agents Chemother.* 2009; 53:3860–3870.
5. Doyle J, Prussia A, White LK, Sun A, Liotta DC, Snyder JP, Compans RW, Plemper RK. Two domains that control prefusion stability and transport competence of the measles virus fusion protein. *J. Virology.* 2006; 80:1524–1536. [PubMed: 16415028]
6. Yoon J-J, Chawla D, Paal T, Ndungu M, Du Y, Kurtkaya S, Sun A, Snyder JP, Plemper RK. High-throughput screening Based Identification of Paramyxovirus Inhibitors. *J. Biomol Screen.* 2008; 13:591. [PubMed: 18626114]
7. 22407448 is called BM-1 through the following parts of the paper for simplicity.
8. Krumm SA, Ndungu JM, Dochow M, Yoon J-J, Sun A, Natchus M, Snyder JP, Plemper RK. Host-Directed Small-Molecule Inhibitors of Myxovirus RNA-dependent RNA-polymerases. *PLoS ONE*. Epublished 16 May 2011 10.1371/journal.pone.0020069.
9. Moyle, G.; Boffito, M.; Shen, Z.; Manhard, K.; Sheedy, B.; Hingorani, V.; Nguyen, M.; Nguyen, T.; Quart, B.; Yeh, L.; Ong, V. RDEA806, a novel HIV nonnucleoside reverse transcriptase inhibitor, shows positive outcome in treatment of naïve HIV patients.. 48 Annual ICAAC/IDSA 46th Annual Meeting; Washington D.C.. 2008;
10. Rosa M, De La, Kim HW, Gunic E, Jenket C, Boyle U, Koh Y, Korboukh I, Allan M, Zhang W, Chen H, Xu W, Nilar S, Yao N, Hamatake R, Lang SA, Hong Z, Zhang Z, Girardet Jean-L. Z. Tri-substituted triazoles as potent non-nucleoside inhibitors of the HIV-1 reverse transcriptase. *Bioorg. Med.Chem. Lett.* 2006; 16:4444–4449. [PubMed: 16806925]
11. Conformational searches of the S, O, NH and CH₂ analogs were performed with the OPLS-2005 force field, and a putative binding model was compared with the global minimum in each case.

Lay Summary

Drugs targeted to viral proteins are highly vulnerable to the development of viral resistance. High-throughput screening previously identified benzimidazole 22407448 with broad anti-viral activity against different influenza virus and paramyxovirus strains. Hit to lead chemistry has generated JMN3-003 with potent antiviral activity against a panel of myxovirus family members including influenza and measles.

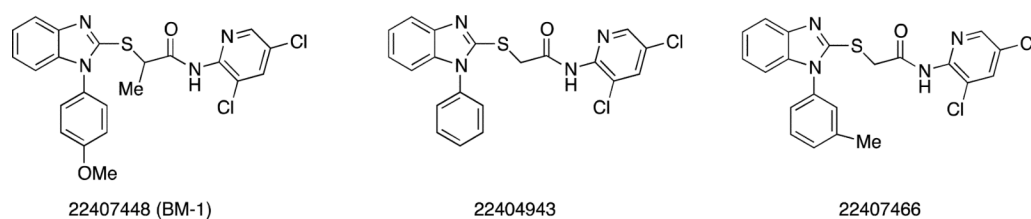
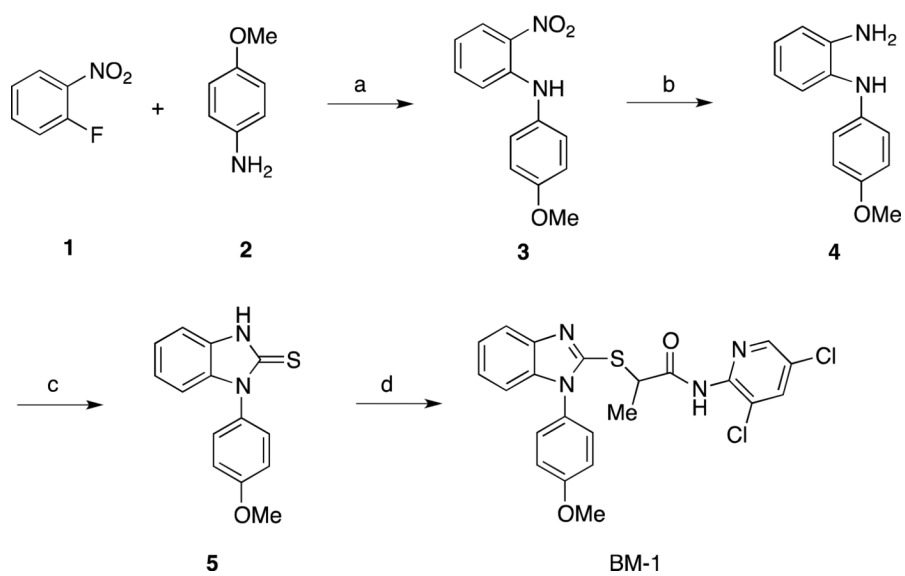


Figure 1.
Anti-MeV hits identified by high-throughput screening.



Scheme 1.
Synthesis of screening hit BM-1^a

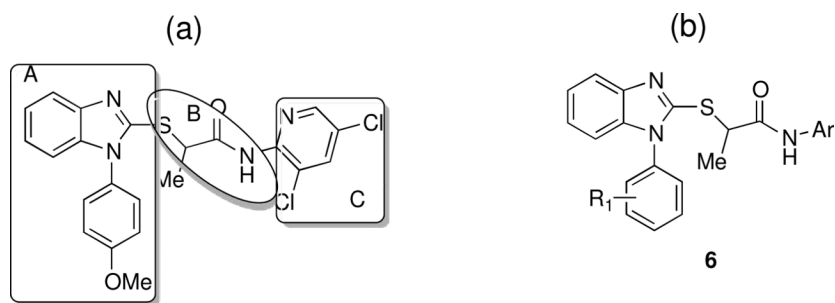


Figure 2.

(a) Structure-activity modification strategy for hit compound BM-1; (b) modification of A and C sectors of BM-1.

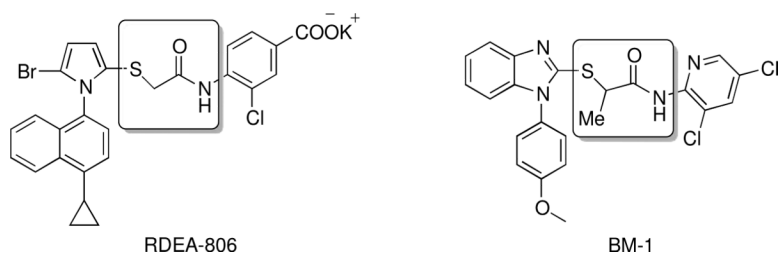
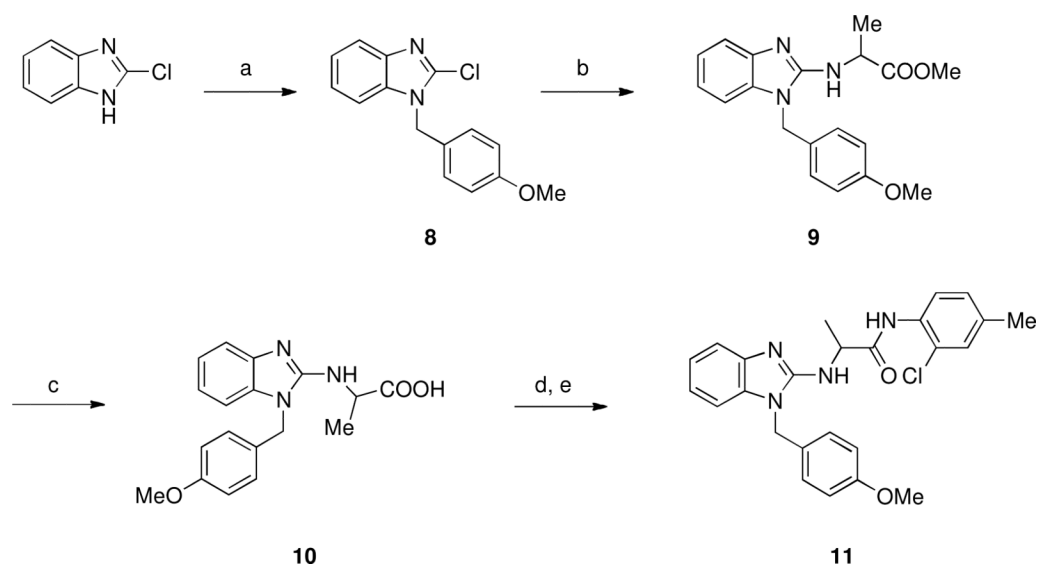
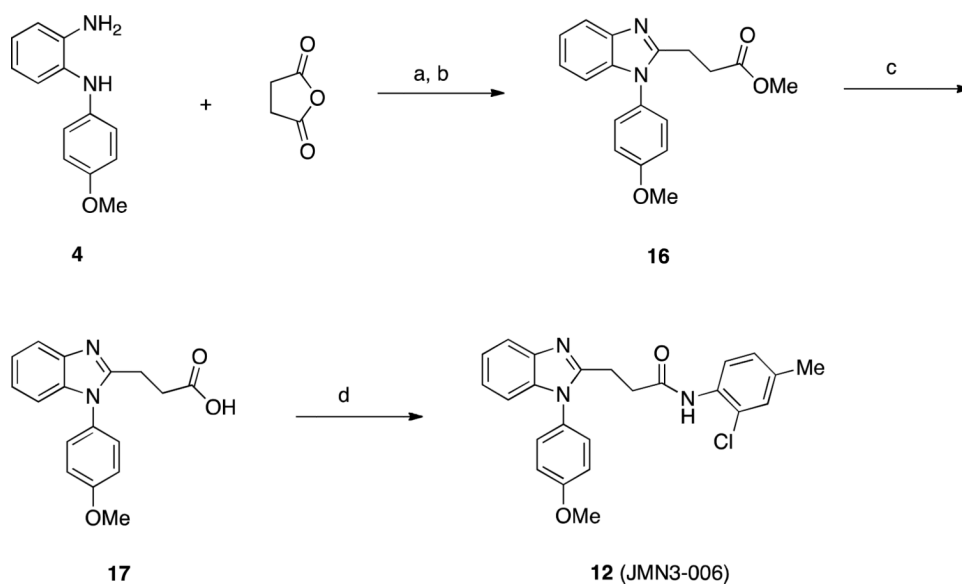


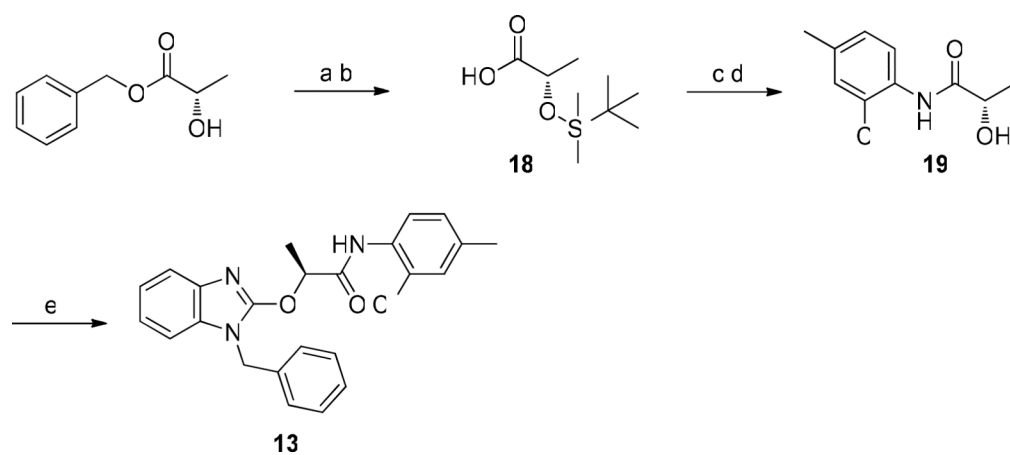
Figure 3.
Structural comparison of RDEA-806 and BM-1.



Scheme 2.
Synthesis of 2-aminobenzimidazole^a



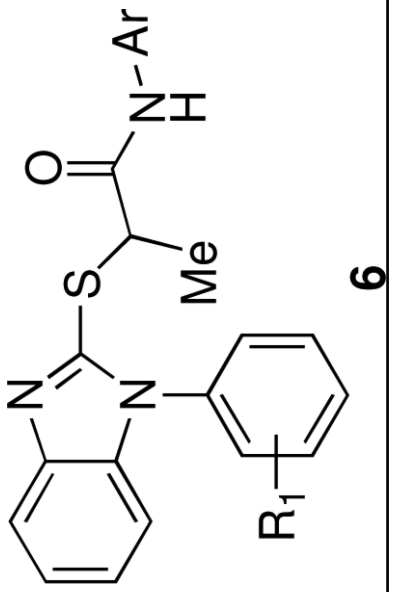
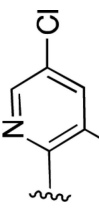
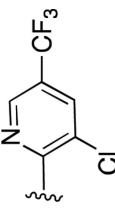
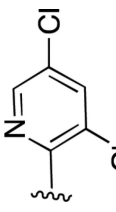
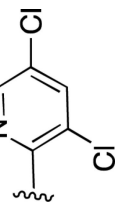
Scheme 3.
Synthesis of the carbon analog of **6p^a**

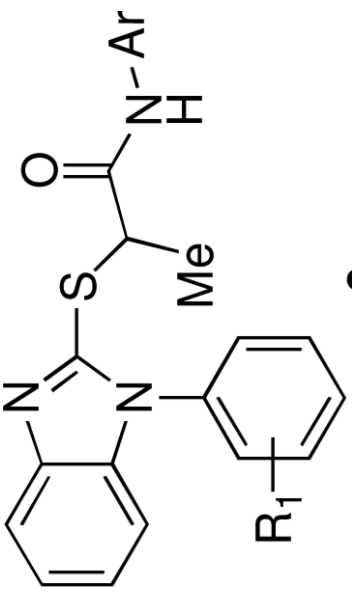
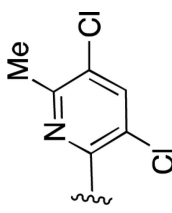
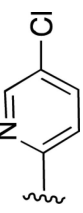
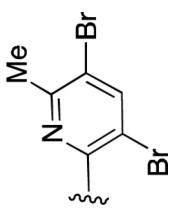
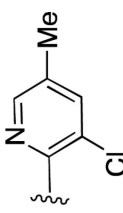


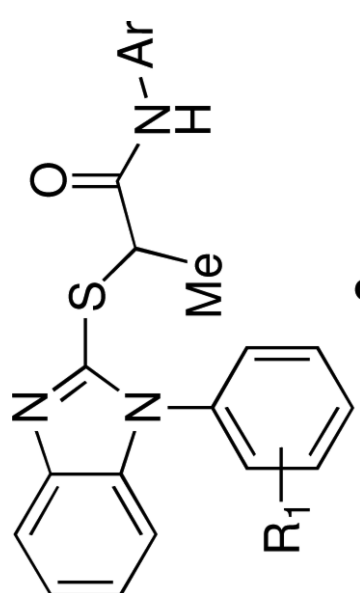
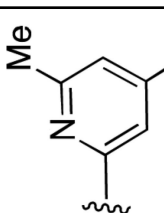
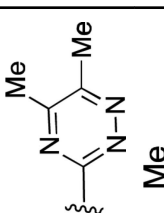
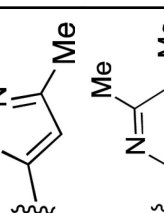

Scheme 4.
Synthesis of the oxygen analog of **6p^a**

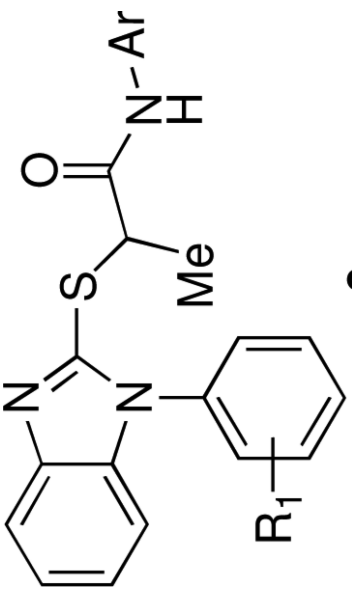
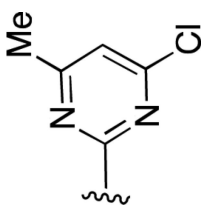
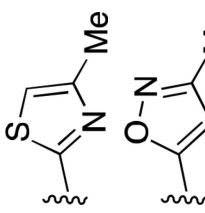
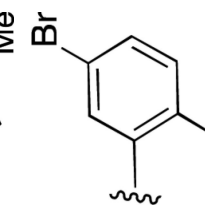

Table 1

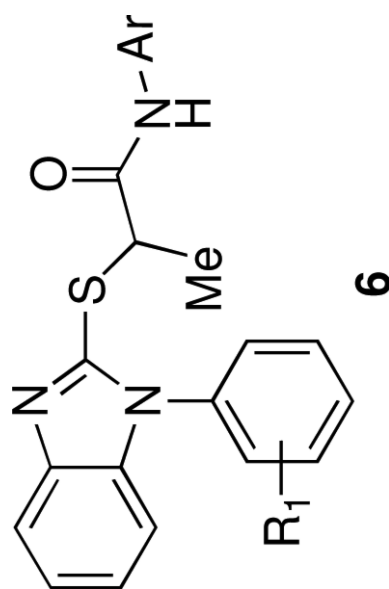
Antiviral activity and cytotoxicity of various substituted anilides **6**.

 6					
Entry	Comp.	R ₁	Ar	EC50 ± SEM (μM) ^a (MeV-Alaska) CPE inhibition	CC ₅₀ (μM) ^b (Vero cells)
hit	BM-1	<i>p</i> -OMe		0.35±0.03	>75
6a	AS92	<i>p</i> -OMe		0.4±0.05	9.2-9.8
6b	AS93	<i>p</i> -F		0.1±0.00	5.9-6.2
6c	AS94	<i>p</i> -OEt		0.1±0.01	18.5-22.2

 6						
Entry	Comp.	R ₁	Ar	EC ₅₀ ± SEM (μM) ^a (MeV-Alaska) CPE inhibition	CC ₅₀ (μM) ^b (Vero cells)	
6d	AS102	<i>p</i> -OMe		0.2±0.01		7.25-7.8
6e	AS80b	<i>p</i> -OMe		>75		ND ^c
6f	AS103b	<i>p</i> -OMe		0.5±0.05		9.7-11.9
6g	AS103a	<i>p</i> -OMe		0.05±0.00		0.88-0.92

 6					
Entry	Comp.	R ₁	Ar	EC ₅₀ ± SEM (μM) ^a (MeV-Alaska) CPE inhibition	CC ₅₀ (μM) ^b (Vero cells)
6h	AS109	<i>p</i> -OEt		1.2±0.22	ND ^c
6i	AS112	<i>p</i> -F		17.4±6.11	ND ^c
6j	AS114	<i>p</i> -OMe		0.5±0.09	75
6k	AS115a	<i>p</i> -OMe		9.3±2.65	ND ^c

 6						
Entry	Comp.	R ₁	Ar	EC50 ± SEM (μM) ^a (MeV-Alaska) CPE inhibition	CC ₅₀ (μM) ^b (Vero cells)	
6l	AS120	<i>p</i> -OMe		>75		ND ^c
6m	JMN2-173	<i>p</i> -OMe		2.8±0.17		ND ^c
6n	JMN2-183	<i>p</i> -OMe		0.4±0.01		>75
6o	AS86	<i>p</i> -OMe		1.4±0.11		ND ^c



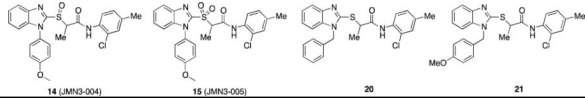
Entry	Comp.	R ₁	Ar	EC ₅₀ ± SEM (μM) ^a (MeV-Alaska) CPE inhibition	CC ₅₀ (μM) ^b (Vero cells)
6p	JMN3-003	<i>p</i> -OMe		0.2±0.00	>75
(S)-6p	(s)-JMN3-003	<i>p</i> -OMe	—	0.3±0.07	>75
(R)-6p	(r)-JMN3-003	<i>p</i> -OMe	—	0.2±0.03	>75

^a 50% inhibitory concentration were calculated using the variable slope (four parameters) non-linear regression-fitting algorithm embedded in the Prism 5 software package (GraphPad Software). Values represent averages of four experiments ± SEM (standard error of the mean); highest concentration assessed, 75 μM.

^b CC₅₀ values represent range of two experiments; highest concentration assessed 75 μM.

^c CC₅₀ not determined (ND) when EC₅₀ > 1.0 μM

Table 2Anti-MeV EC₅₀ values for S-atom replacements

			
ID	Comp.	EC ₅₀ (μM) ^a (MeV-Alaska)	CC ₅₀ (μM) ^b (Vero cells)
11	AS-228	> 150	ND ^c
12	JMN3-006	>150	ND
13	JMN8-096	>150	ND
14	JMN3-004	1.3±0.06	>75
15	JMN3-005	>150	ND
20	JMN5-010	0.4±0.06	>75
21	JMN4-023	0.7±0.04	>75

^a 50% inhibitory concentration were calculated using the variable slope (four parameters) non-linear regression-fitting algorithm embedded in the Prism 5 software package (GraphPad Software). Values represent averages of four experiments± SEM (standard error of the mean); highest concentration assessed, 75 μM.

^b values represent averages of two experiments; highest concentration assessed 75 μM

^c CC₅₀ not determined (ND) when EC₅₀ >150 μM